Infrared Spectroscopic Studies of Surface Properties of Mo/SnO$_2$ Catalyst

Marco Daturi* and Lucia Gorenstin Appel†,[1]

*Laboratoire de Catalyse et Spectrochimie, UMR 6506, ISMRA, 6, Boulevard du Maréchal Juin, 14050, Caen Cedex, France; and †Laboratório de Catálise, Instituto Nacional de Tecnologia, Av. Venezuela 82/sala 518, CEP 20081-310, Rio de Janeiro, Brazil

Mo/SnO$_2$ catalysts to be used for catalytic oxidation of ethanol and SnO$_2$ were characterized by FTIR using pyridine, carbon monoxide, and methanol as probe molecules. Adding Mo to SnO$_2$ does not modify the acidity of SnO$_2$, but it decreases the number of acid centers. It was observed that in the process of drying the Mo/SnO$_2$, Mo-isolated tetrahedral species developed on the surface of SnO$_2$. These species are formed by the reaction of Mo$_7$O$_{24}^{2-}$ with basic hydroxyl species and probably also with Lewis acid sites. It was possible to observe two kinds of alcooxides at least. One of them is adsorbed on the oxygen of the Mo=O molybdenil unit and the other on hydroxyl species. The former is active for ethanol oxidation and the latter promotes the formation of by-products. © 2002 Elsevier Science (USA)

Key Words: ethanol; molybdenum; tin; oxidation; methanol; pyridine; Lewis acidity; alcooxides; hydroxyls.

INTRODUCTION

Acetic acid is currently produced from ethanol by dehydrogenation to acetaldehyde in the gas phase and subsequent oxidation in the liquid phase. Using two reactors for this process consequently increases costs. Moreover, the dehydrogenation catalysts tend to deactivate, while environmental problems are associated with the homogeneous systems. Previous studies have shown that Mo/SnO$_2$ systems are very selective for producing acetic acid from ethanol oxidation in a single step (1, 2). They also indicated that acetaldehyde is the primary product, which is then oxidized to acetic acid and carbon oxides. It was shown that it is necessary to attain complete conversion of ethanol to produce acetic acid and carbon dioxide from acetaldehyde (1, 3).

Moreover, Mo/SnO$_2$ catalysts are very promising for the oxidative dehydrogenation of alcohols, the first step of the acid acetic production. They show higher activity than Mo/TiO$_2$, Mo/Al$_2$O$_3$, and Mo/SiO$_2$ catalysts (4). As described below, this catalytic behavior has been interpreted from different points of view.

Moro-oka (5) related the catalytic performance of Mo/SnO$_2$ systems in selective oxidation to their acid prop-

erties. Indeed, Niwa and Igarashi (6) claimed that acidity plays an important role in the oxidative dehydrogenation of methanol. These authors correlated the catalytic behavior of Mo/SnO$_2$ systems to the presence of acid sites, possibly Brønsted sites, located on molybdenum oxide supported on tin oxide. However, Okamoto *et al.* (7), studying the oxidative dehydrogenation of *sec*-butyric alcohol for systems with low Mo concentration (Mo/Mo + Sn < 0.5), suggested that the catalytic activity of the Mo/SnO$_2$ system might be associated with the dissolution of Mo in the SnO$_2$ crystal.

On the other hand, Zhang *et al.* (8) and Hangchun and Wachs (9), studying the oxidative dehydrogenation of alcohol, suggested that the activity of the catalyst should depend upon the reducibility of the support associated with the availability of empty electronic states in the intermediate surface complex. In this context, Gonçalves *et al.* (1) proposed that the higher catalytic activity of the Mo/SnO$_2$ system compared to that of the above-mentioned supports was due to a greater reducibility of SnO$_2$. Taking into account characterization and tests on these materials prepared by different procedures, the same authors proposed that the catalytic activity of these materials on oxidative dehydrogenation of ethanol was associated with the presence of Mo isolated species of tetrahedral coordination. In addition they observed that condensed species, such as molybdates and MoO$_3$, showed low activity for this reaction.

From previous work, it appears that there is no agreement about the properties that influence the catalytic activity of the Mo/SnO$_2$ system in ethanol oxidation. This may be attributed to the nonavailability of a complete characterization of this system. The objective of this work is to contribute to the identification of the physicochemical characteristics of the Mo/SnO$_2$ system that could influence its catalytic behavior in the oxidative dehydrogenation of alcohols, through an infrared spectroscopic investigation.

EXPERIMENTAL

Preparation

The Mo/SnO$_2$ systems were obtained from the precipitation, in aqueous solution, of SnO$_2 \cdot x$H$_2$O in the presence of (NH$_4$)$_2$Mo$_7$O$_{24}$ (HMA). This precipitation was the

[1] To whom correspondence should be addressed. Fax: 55 21 22636552. E-mail: appel@uol.com.br.

result of the slow addition of solutions of NH_4OH and $SnCl_4$ to a solution of HMA, followed by evaporation. The pH value during the precipitation was fixed at 10. The solids were dried in the oven at 110°C and calcined at 500°C in a muffle for 16 h. The preparation of SnO_2 followed the same procedures used in the case of the catalyst, without Mo salt being added during the precipitation. Low concentrations of Mo samples were synthesized in order to minimize the number of Mo species present in the catalyst.

Characterization

Infrared spectroscopy analyses were performed using a Magna 750-Nicolet apparatus. Catalyst samples of approximately 11 mg · cm^{-2} were pressed into a thin wafer and used for adsorption of CO, pyridine, and methanol. The Mo/SnO_2 and SnO_2 wafers mass were 16.9 and 22.7 mg, respectively. The wafers were activated by drying, treated at 500°C for 20 min under 100 Torr of O_2, evacuated to 10^{-6} Torr at 500°C for 30 min, and finally cooled to room temperature, before adsorption of the probe molecules. The FTIR results were normalized to the mass of the wafers. The choice of methanol as probe molecule was associated with previous experiments, which indicate that this molecule is sensitive to the identification of cationic sites present on the catalyst surface (10). The results obtained by methanol adsorption were considered useful in the interpretation of data concerning ethanol oxidation, considering the chemical similarity between the two substances.

Measurements of specific area and chemical analyses were carried out by BET technique, using CG 2000 equipment, and by X-ray fluorescence spectroscopy, using Philips PW 2400 equipment.

Catalytic Tests

The catalytic tests for ethanol oxidation were performed in a conventional system using a fixed-bed reactor and monitored by online gas chromatography, with flame ionization and conductivity detectors. The rate values were obtained under ethanol isoconversion (10%) at 150°C, with a 3% ethanol/air mixture. No deactivation of the catalysts was observed during the study.

RESULTS

The values of surface area and the reaction rate of Mo/SnO_2 and SnO_2 are reported in Table 1. As can be observed, the presence of Mo increased the surface area of SnO_2, which indicates a modification of the texture of this oxide by interaction with molybdenum, as was previously observed (1).

The results of the catalytic test in ethanol oxidation at 150°C show that the selectivity of Mo/SnO_2 to acetaldehyde is 75%. Other compounds, such as ethyl acetate, ethyl ether, and ethylene, have been detected; their selectivities

TABLE 1

Values of Mo Concentration, Specific Surface Area (S), and Rate of Ethanol Oxidation at 150°C (R)

Catalysts	Mo (wt%)	S (m^2/g)	R (μmol ethanol · m^{-2} · h^{-1})
SnO_2	—	34	—
Mo/SnO_2	3.2	65	50.1

are around 9, 6, and 5%, respectively. Other compounds can also be observed at lower concentrations. They are acrolein, furan, ethyl formate, and methyl acetate.

We also investigated a possible contribution of the support to the activity. In spite of using a SnO_2 mass 15 times higher than that of the Mo/SnO_2 catalyst, we found no evidence of conversion due to SnO_2. This result shows that the catalytic activity of the Mo/SnO_2 system under these conditions is due to the presence of Mo species.

Figure 1 displays the pyridine adsorption study on Mo/SnO_2 catalyst and on SnO_2. Two main bands are observed, at 1450 and 1615 cm^{-1}, which are attributed to Lewis acid sites on both materials (11). It is reported that ring vibration mode frequencies are more or less shifted by the interaction of pyridine with surface Lewis acid centers, with the 8a mode being the most sensitive (12). The 8a mode is located at 1583 cm^{-1} for liquidlike (van der Waals) physically adsorbed pyridine (10, 11) (Fig. 1e) and is shifted upward by pyridine adsorption on Lewis centers according to their acid strength. In the case of the SnO_2 and Mo/SnO_2 catalysts, shifts are identical for both samples and equal to 32 cm^{-1} (from 1583 up to 1615 cm^{-1}). This result suggests
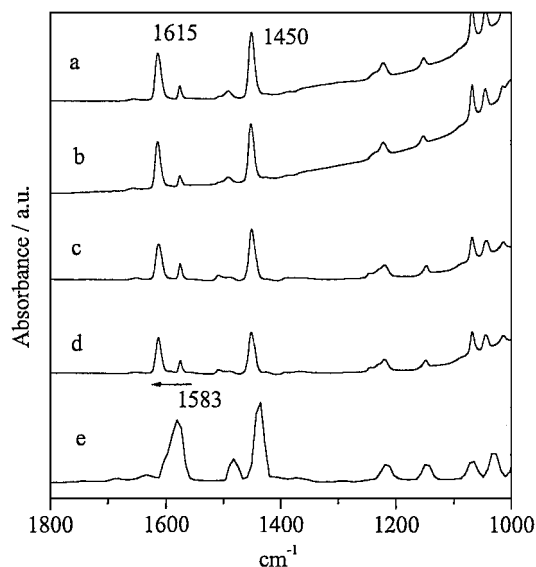

FIG. 1. Infrared spectra after pyridine adsorption and evacuation on Mo/SnO_2 at 25°C (a), 100°C (b), on SnO_2 at 25°C (c), and 100°C (d). Spectrum of pyridine (liquid) (e).

that the presence of Mo does not change the features of the acid sites present on SnO_2. Moreover, the literature reports that CeO_2, TiO_2, and ZrO_2 give shifts of 10, 27, and 23 cm^{-1}, respectively (10). Thus SnO_2 and Mo/SnO$_2$ Lewis sites show an acid strength higher than that previously observed by pyridine adsorption on the mentioned oxides, even if well below that of γ-Al$_2$O$_3$, which presents the 8a mode at 1625 cm^{-1} (shift of 42 cm^{-1}) (12, 13). Figure 1 displays also the spectra (b and d) obtained after heating the samples at 100°C under vacuum, which are quite similar to those obtained at 25°C. This fact is in agreement with the observations cited above relating to the acid strength of the sites involved, showing that the probe coordination molecule is stable upon evacuation at increasing temperature. Moreover, the spectra do not show features near 1540 cm^{-1}, which is attributed to Brønsted acid sites, and thus suggests the absence of such acid sites on our samples.

Concerning the intensity of the bands (proportional to the density of the exposed acid sites), it may be observed that the ratio in peak areas at 1615 cm^{-1} of the Mo/SnO$_2$ catalyst to that of the bare SnO$_2$ (spectra a and c and spectra b and d in Fig. 1) is 1.3. However, when these values are standardized in relation to the specific surface area, it was calculated that the Mo/SnO$_2$ catalyst presents a population of acid sites 33% smaller than that of SnO$_2$.

The adsorption of CO (basic probe) may also be used to characterize Lewis acidity of the catalysts (14). Indeed CO acts as a σ-electron donor through its 5σ orbital mainly localized on C atoms. Thus, it probes the Lewis acid sites on the catalyst. Using the 2143-cm^{-1} value for the ν(CO) mode in gaseous CO as a reference (10, 11), the extent of the upward shift of this vibration wavenumber is commonly used to evaluate the acidity of the cationic adsorption site when CO interacts as a Lewis base. Actually, for both materials, bands related to CO adsorption are observed around 2200 cm^{-1} (Fig. 2) showing the presence of Lewis acid sites of equal strength. These results also confirm that Mo does not alter the acidity of the sites present on SnO$_2$, as observed with pyridine adsorption. By comparison of band intensities it was observed, too, that the number of acid sites on SnO$_2$ is higher than that on Mo/SnO$_2$. This result can be ascribed to the presence of the supported molybdenum, which partially occupies surface sites.

Figure 3 displays Mo/SnO$_2$ infrared spectra recorded in the 1200- to 800-cm^{-1} range. In Fig. 3a two broad bands, one at 964 and the other at 860 cm^{-1}, can be observed for Mo/SnO$_2$ catalyst with no treatment. Indeed, absorptions in the 920- to 1010-cm^{-1} range are associated with the stretch of the Mo=O bond, already extensively studied in the case of Mo-supported catalysts (15, 16). As a matter of fact, bands at 990 cm^{-1} are attributed to crystalline MoO$_3$ (17). Mo-dispersed species, i.e., polymolybdates and isolated hydrated tetrahedral species, show ab-
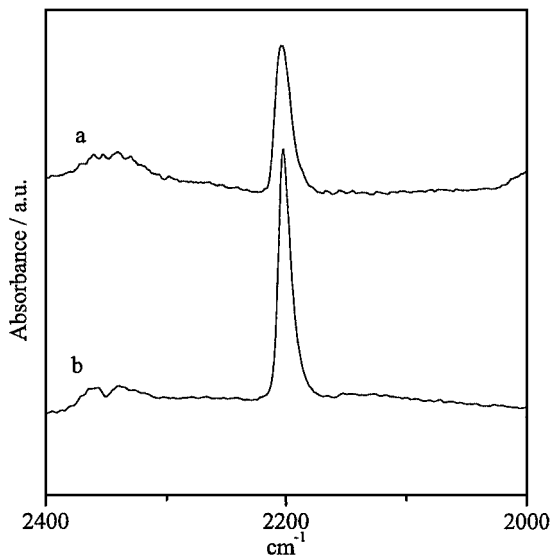

FIG. 2. Infrared spectra after CO adsorption (10 Torr) on Mo/SnO₂ (a) and on SnO₂ (b) at room temperature.

sorptions around 964 cm^{-1}, attributed to Mo=O (15). Even if these species are intrinsically different, the nature of the Mo=O bond is the same, which results in absorptions with similar wavenumbers. On the other hand, the vibration at 860 cm^{-1} may be associated with Mo–O–Mo (16) or even to Mo–O–Sn stretching modes. The latter is based on Kasztelan *et al.* (18), who assigned for Mo/Al$_2$O$_3$ systems with low Mo concentrations a vibration is due to
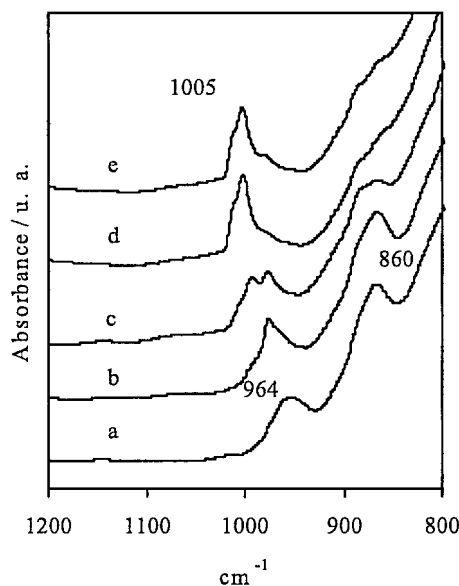

FIG. 3. Infrared spectra of Mo/SnO₂ without treatment (a), evacuated at 10⁻³ Torr at 25°C (b), evacuated at 10⁻³ Torr at 500°C during 20 min (c), evacuated at 10⁻⁸ Torr at 500°C during 25 min (d), after 100 Torr O₂, 25°C during 5 min (e).

Mo–O–Al bonds in this region. It is important to stress that the Mo–O–Mo unit is associated with polymolybdates, while Mo–O–Sn is related to isolated tetrahedral Mo species. Therefore FTIR results do not allow these two kinds of coordinations at hydrated conditions to be distinguished.

Figures 3b–3e display the behavior of the Mo=O vibration during the drying process. As the sample is being dried, this vibration, at 964 cm^{-1}, decreases in intensity and another feature appears at 1005 cm^{-1}. This modification has been previously observed for Mo-supported catalysts on different oxides (16, 19) and it has been explained by structural alterations in the Mo species. According to Desikan *et al.* (16), this phenomenon would indicate the presence of isolated tetrahedral Mo species, which are present in an octahedral coordination in the presence of water. This result is in agreement with previous observations by UV spectrometry and through Mo surface measurements (1). It is worth pointing out that the vibration at 860 cm^{-1}, which should be associated with the stretch of the Mo–O–Sn bonds, reduces in intensity during the drying process.

Figure 4 displays Mo/SnO$_2$ catalyst and SnO$_2$ infrared spectra recorded in the 3000- to 4000-cm^{-1} range after specific treatment of the samples. As can be observed, SnO$_2$ presents three main bands, at 3716, 3668, and 3208 cm^{-1}. The first two (Fig. 4a) are assigned to surface hydroxyl species, while the last is typical of N–H bond vibrations, which might be related to residues of ammonium salts used 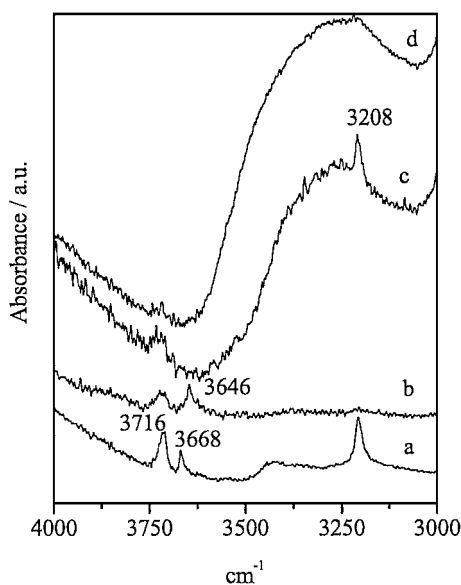during the preparation. The spectrum related to the Mo/SnO$_2$ (Fig. 4b) shows the presence of two main bands, one at 3719 and the other at 3646 cm^{-1}. The last one is shifted compared to the SnO$_2$ sample. The ratio between the intensities of hydroxyl species on SnO$_2$ and on the Mo/SnO$_2$ catalyst are 2.40 and 1 for the 3719 and 3646 cm^{-1} features, respectively. The absorption values were normalized with the mass of the wafer and taking into account the surface area. Therefore, it may be concluded that the anchoring of Mo on the surface of SnO$_2$ has occurred to the detriment of OH sites of SnO$_2$ having higher, thus more basic, wavenumbers. The explanation is in agreement with the higher reactivity of Mo toward basic hydroxyls already described for alumina (20). The absence of any band assigned to the ν(N–H) bond vibration on the support (3208 cm^{-1}), can also be observed. As the thermal treatments were identical for both samples, it may be inferred that during preparation Mo competes with the same sites as the N impurities, thus displacing them, or that the presence of the metal favors nitro compound decomposition. The presence of these species on the surface of SnO$_2$ should be related to the existence of Lewis acid sites and to their decrease in density when molybdenum is present, as reported above for pyridine and CO adsorption tests.

Figure 4 also displays the spectra concerning methanol adsorption on SnO$_2$ and on Mo/SnO$_2$ catalyst, in the 3000- to 4000-cm^{-1} range (spectra c and d). Figure 4c shows that methanol adsorption on SnO$_2$ competes with hydroxyl species. This result is in agreement with a dissociative adsorption of the alcohol: the formation of methoxy groups takes place on the same sites as hydroxyls, since they both compensate for the coordinative unsaturation of the cations at the surface of the solids (21). The broad band in the 3500- to 3200-cm^{-1} region can be ascribed to water formation coming from the hydrogen coordination with OH groups after methanol dissociation.

Also in the case of the Mo/SnO$_2$ catalyst, the adsorption of methanol (Fig. 4d) provokes the almost total consumption of the hydroxyl species and the appearance of a band related to water, as already described for SnO$_2$ (4c).

Figure 5b displays bands associated with the adsorption of methanol on SnO$_2$ in the 800- to 1200-cm^{-1} range (ν(OC) stretching region), in comparison to the sample surface activated under oxygen displayed in Fig. 5a. The main feature is a broad band located at 1067 cm^{-1}. Figure 5c shows Mo/SnO$_2$ catalyst activated under oxygen. Figure 5d, related to the adsorption of methanol on the Mo/SnO$_2$ sample, shows a broad massif with maxima at 1054 and 970 cm^{-1}. The deconvolution (Fig. 5e) of this feature puts in evidence five bands, at 1066, 1052, 1019, 996, and 969 cm^{-1}. The analysis of Fig. 5b (methanol on SnO$_2$) gives a broad band around 1067 cm^{-1} with others of lower intensity, so that the feature at 1066 cm^{-1} could be assigned to the ν(O–C) vibration of methoxy species related to the dissociative adsorption of methanol on Sn^{4+} sites. On the other

FIG. 4. Infrared spectra of SnO$_2$ at 25°C after treatment at 500°C during 20 min under 100 Torr of O$_2$, followed by evacuation (10^{-8} Torr), at 500°C during 30 min (a), the same pretreatment but for Mo/SnO$_2$ (b), SnO$_2$ spectrum after 1 Torr methanol adsorption during 15 min (c) and Mo/SnO$_2$ spectrum after the same procedure as spectrum c (d).
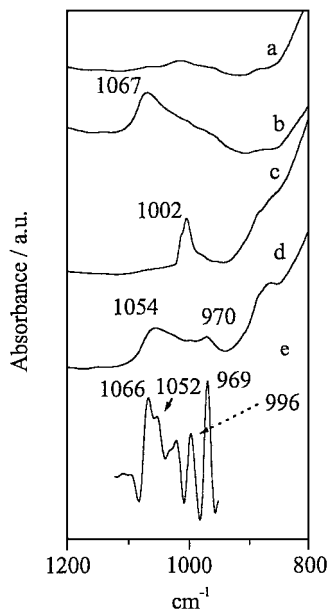
FIG. 5. Infrared spectra of SnO₂ at 25°C after treatment at 500°C during 20 min under 100 torr of O₂, followed by evacuation (10⁻⁸ Torr) at 500°C during 30 min (a), SnO₂ after 1 Torr methanol adsorption at 25°C during 15 min (b), the same treatment as spectrum a for Mo/SnO₂ (c), Mo/SnO₂ after 1 Torr methanol adsorption at 25°C during 15 min (d), deconvolution of spectrum d (e).

hand, Groff reported a band around 1065 cm⁻¹ for the adsorption of methanol on MoO₃ as well (22). Taking into account the fact that there might be some differences between the adsorption of methanol on Mo dispersed species and on MoO₃, it might be suggested that the component at 1066 cm⁻¹ of Fig. 5e is anyway related to the adsorption of methanol on SnO₂, while the band at 1052 cm⁻¹ might be assigned to the adsorption of methanol on molybdenum sites that could present here, as a dispersed phase, a more metallic character than is found in the bulk oxide form. This consideration will justify wavenumber lowering. The band at 1019 cm⁻¹ might be associated with the vibrations of Sn–O bonds or, alternatively, with traces of undissociated methanol. The 996- and 969-cm⁻¹ contributions are assigned to the vibration of Mo=O units, dry and hydrated, respectively, as discussed above. In fact, the adsorption of methanol has generated water on the surface of the Mo/SnO₂ sample, hydrating some remaining Mo sites and causing a shift in the band related to molybdenil vibration (Mo=O). Comparing Figs. 5c and 5d one may infer that methanol adsorption occurs on the most exposed sites, by breaking the Mo=O bond, which is in agreement with the information in the literature (23).

DISCUSSION

Davidov (24) observed that low concentrations of Mo did not change the acidity of SnO₂. The same author suggested

that the Brønsted acidity observed in the Mo/SnO₂ systems with high Mo concentration may be related to the presence of MoO₃. On the other hand, data previously obtained (1) showed that the activity of the Mo/SnO₂ system cannot be associated with MoO₃, since this species presents low catalytic activity in the oxidation of ethanol compared to that of Mo dispersed species. Besides this fact, the Mo low content samples here studied, which as FTIR results pointed out are free from MoO₃, present significant activity in the ethanol oxidation. Moreover the results show that SnO₂ and Mo/SnO₂ have the same kind of acid sites, but Mo/SnO₂ has a number of sites per unit area lower than SnO₂. Thus the results here obtained differ from those published by Niwa and Igarashi (6), who proposed that the acid sites, located on molybdenum oxide supported on tin oxide, are responsible for the catalytic activity of the Mo/SnO₂ system in the oxidative dehydrogenation of alcohols. Indeed, the increase in activity given by Mo addition to SnO₂ cannot be connected to the acidity enhancement.

Previous work (1, 25) has shown that Mo/SnO₂ catalysis, depending on preparation procedure and Mo loading, may show MoO₃, tridimensional polymolybdates, and Mo-isolated tetrahedral species. It was found that the last one, the 4-coordinated species, are up to 10 times more active than the 6-coordinated ones in the reaction of oxidative dehydrogenation of ethanol and, moreover, are twice more selective for acetic acid at high ethanol conversion. In addition, the highly reducible SnO₂ support provides catalysts up to four times more active in ethanol oxidative dehydrogenation than those obtained with TiO₂, which is more active than Al₂O₃ or SiO₂. Indeed our previous results (1) suggested that the higher dispersion on a highly reducible support leads to more-active catalysts by optimizing the interaction with the support. The results here presented postulate the presence of isolated Mo species. These species seems to be the only form in which molybdenum is present in the catalytic system. Therefore, the catalytic activity observed in ethanol oxidation (Table 1) may be associated with them.

Mo-isolated species have been observed to have tetrahedral coordination, which demands the generation of two bonds, Sn–O–Mo. Segawa and Hall (20), studying the Mo/Al₂O₃ system, suggest that the formation of these entities might be associated with the reaction of Mo with basic and neutral hydroxyls of the support. However, the results of this study suggest that the creation of these Mo species on SnO₂ involves basic hydroxyls and Lewis acid sites.

Alcohol oxidative dehydrogenation catalyzed by Mo is an extensively studied reaction (23). It is sensitive to the structure (26) and occurs via an alcooxide-type intermediate, which is transformed into an aldehyde. The rate-determining step involves the extraction of hydrogen from the adsorbed alcooxide group. Indeed, the metallic cation that adsorbs the ethoxide should be able to receive

electrons or to be reduced (23). The results obtained indicate the presence of at least two kinds of methanol adsorption sites associated with Sn and Mo. TPR results previously obtained (1) showed that surface Mo (isolated tetrahedral dispersed species) are more easily reduced than the Sn (SnO_2). Therefore both ethoxides seem to be able to generate acetaldehyde, being the catalyst most active due to the presence of Mo. On the other hand, the presence of Lewis acids sites on the support and the adsorption of alcooxides cause secondary reactions, generating by-products such as ethyl acetate, ethyl ether, and ethylene, which decrease the selectivity of the reaction for acetaldehyde formation.

CONCLUSIONS

The presence of isolated Mo tetrahedral species on SnO_2 has been confirmed by this IR study. These species are anchored on the surface of SnO_2 through a reaction of the Mo salt with the surface basic hydroxyls and possibly with Lewis acid sites. It was possible to observe at least two kinds of alcooxides, one of them adsorbed at the place of O by breaking the Mo=O bond and the other replacing hydroxyl species coordinated with tin. It is proposed that the former is active for ethanol oxidation and the latter promotes the formation of by-products. This study is in agreement with the concept of catalytic site isolation (27, 28).

ACKNOWLEDGMENTS

REFERENCES

1. Gonçalves, F., Medeiros, P. R. S., Eon, J. G., and Appel, L. G., *Appl. Catal. A* **193**(1–2), 195 (2000).
2. Allakhverdova, N. Kh., Adzhamov, K. Yu., and Alkhazov, T. G., *Kinet. Katal.* **33**, 586 (1992).
3. Medeiros, P. R., Eon, J. G., and Appel, L. G., *Catal. Lett.* **69**, 79 (2000).
4. Niwa, M., Sano, M., Yamada, H., and Murakami, Y., *J. Catal.* **151**, 285 (1995).
5. Moro-oka, Y., *Appl. Catal. A* **181**, 323 (1999).
6. Niwa, M., and Igarashi, J., *Catal. Today* **52**, 71 (1999).
7. Okamoto, Y., Oh-Hiraki, K. E., and Teranishi, S., *J. Catal.* **71**, 99 (1981).
8. Zhang, W., Desikan, A., and Oyama, S. T., *J. Phys. Chem.* **99**, 14468 (1995).
9. Hangchun, H., and Wachs, I. E., *J. Phys. Chem.* **99**, 10911 (1995).
10. Binet, C., Daturi, M., and Lavalley, J. C., *Catal. Today* **50**, 207 (1999).
11. Ertl, G., Knözinger, H., and Weitkamp, J., "Handbook of Heterogeneous Catalysis." Wiley–VCH, New York, 1997.
12. Busca, G., *Catal. Today* **41**, 191 (1998).
13. Busca, G., *Phys. Chem. Chem. Phys.* **1**, 723 (1999).
14. Payen, E., Grimblot, J., Lavalley, J. C., Daturi, M., and Maugé, F., "Vibrational Spectroscopy in the Study of Oxide Catalysts (Excluding Zeolites)," Handbook of Vibrational Spectroscopy. Wiley, New York, 2002.
15. Hangchun, H., and Wachs, I. E., *J. Phys. Chem.* **99**, 10897 (1995).
16. Desikan, A. N., Huang, L., and Oyama, S. T., *J. Chem. Soc. Faraday Trans.* **88**, 22 3357 (1992).
17. Niwa, M., Sano, M., Yamada, H., and Murakami, Y., *J. Catal.* **134**, 331 (1992).
18. Kasztelan, S., Payen, E., Toulhoat, H., Grimblot, J., and Bonnelle, J. P., *Polyhedron* **5**, 157 (1986).
19. Hangchun, H., and Wachs, I. E., *J. Phys. Chem.* **99**, 10911 (1995).
20. Segawa, K., and Hall, W. K., *J. Catal.* **76**, 133 (1982).
21. Daturi, M., Binet, C., Lavalley, J.-C., Galtayries, A., and Sporken, R., *Phys. Chem. Chem. Phys.* **1**, 5717 (1999).
22. Groff, R. P., *J. Catal.* **86**, 215 (1984).
23. Tatibouët, J. M., *Appl. Catal. A* **148**, 213 (1997).
24. Davydov, A. A., *React. Kinet. Catal. Lett.* **191**(3–4), 377 (1982).
25. Medeiros, P. R., and Appel, L. G., *Appl. Catal. A* **231**, 125 (2002).
26. Tatibouët, J. M., Germain, J. E., and Volta, J. C., *J. Catal.* **82**, 240 (1983).
27. Grasselli, R. K., *Top. Catal.* **15**(2–4), 93 (2001).
28. Volta, J. C., *Top. Catal.* **15**(2–4), 121 (2001).